LAB - PHYSICAL MODELING OF FLUID

BY

SACHIN SRINIVASA SHETTY

Contents

List of Figures

List of Tables

1 Introduction

In this lab, we are going to perform simulations on test cases NACA0012 wing profile and AGARD Case wing profile using Fine/Marine solver to analyze turbulent flows. The post-processing is performed and the obtained values are validated with the experimental values. The $k-\omega$ SST (Menter) model is implemented for the turbulence problem. The Wall function and the Wall resolved approaches are compared. In the first part of the study, we study the simulations related to the NACA0012 profile. In the second part of the study, we study the simulations related to the AGARD case.

2 Part I:NACA0012 profile at 0° angle of attack

In this section, we are going to study the simulation results based on the profile presented in the below figure. The angle of attack is 0 degrees. The length of the chord is set to unity. The Reynolds number considered are $2X10^6$ and $4x10^6$. The two approaches are Wall function and Wall Resolved. We then perform a grid convergence study. The inlet velocity conditions are set to unity. The density of the fluid is taken as unity. The external boundary conditions, far-field boundary conditions are prescribed for the inlet boundary, Top and bottom, while prescribed pressure is set on the outlet boundaries for all the simulations.

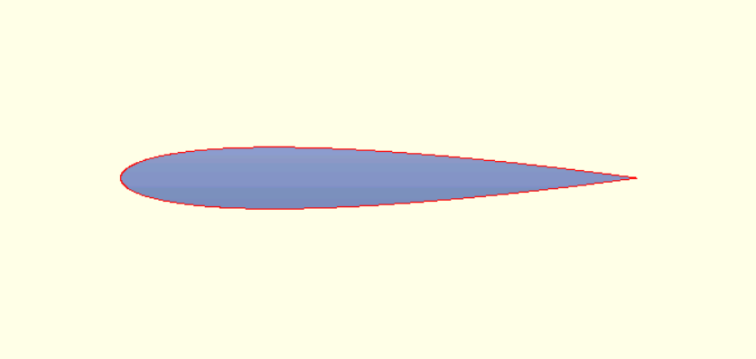

Figure 1: NACA0012 Profile at 0° Angle of Attack

2.1 Wall Function and Wall resolved Approach

In this section,We are going to analyse the results using both the wall function and wall resolved approaches.The below figures shows the different mesh adaptation.

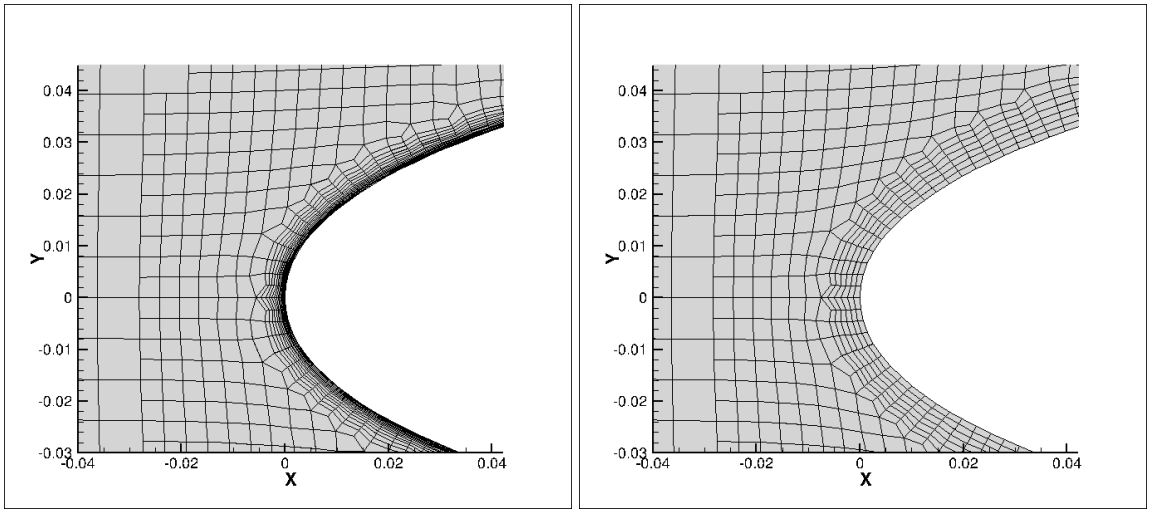

(a) Adapted Mesh to Wall Function

(b) Adapted Mesh to Wall Resolved

Figure 2: Different Mesh adaptation for Medium Mesh,Re=$2x10^6$

2.2 y+ Values,Convergence and the Flow fields

It was observed that both the forces and the residuals of velocity, pressure, turbulent kinetic energy seem to be well converged in all these cases. It can be observed that the wall resolved approach takes a long time to converge compared to a wall function approach which is expected to take less computational effort.

Now the y+ values around the profile are checked to ensure proper wall approaches are being solved and the respective y+ values are acceptable. It has to be ensured that the y+ value for a wall function approach is high enough, around 40, while for a wall resolved approach, the y+ value must be < 1. The medium graded meshes for these cases are adapted using a y+ value of 0.5 for wall resolved, and a y+ value of 40 for wall function approach using appropriate kinematic viscosity based on the Re. As observed in the figures presented, for a wall function approach, the y+ values are mostly around 40 along with the profile and always > 1, while for the wall resolved approach, the y+ values are < 1 everywhere as expected. Thus they are acceptable.

The below-mentioned figure illustrates the evolution of the eddy viscosity and the turbulent kinetic energy around the wing using the two approaches for both the cases of Re. Between, wall function and wall resolved, there is not much of a difference in the results for eddy viscosity. However, in the case of the turbulent kinetic energy, in the wake region, it seems like it diffuses just a bit earlier when the wall function is used compared to its counterpart. In the other case of Reynolds number, the eddy viscosity seems to be a little more intense as expected with higher Re.

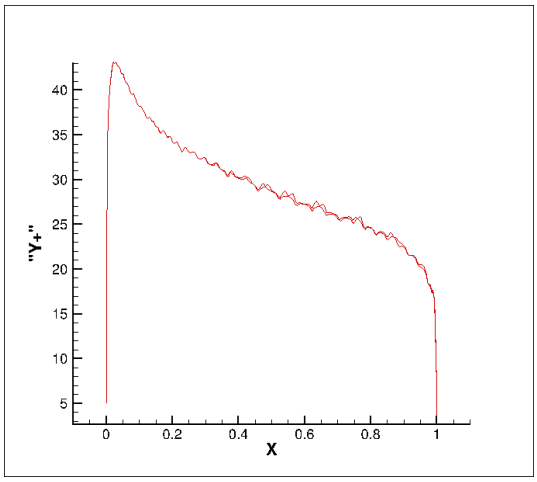

(a) Y+,Wall Function

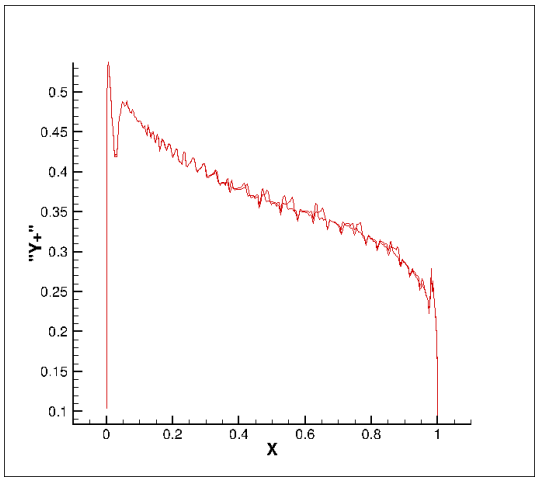

(b) Y+,Wall Resolved

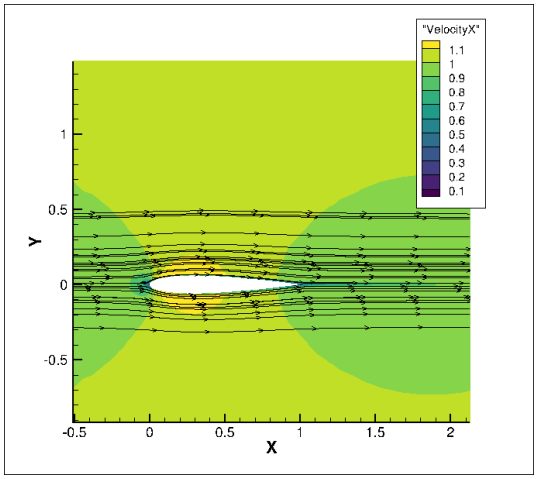

(c) Velocity,Wall Function

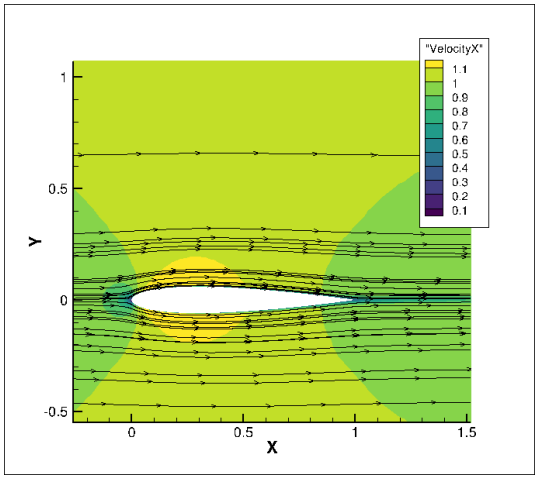

(d) Velocity,Wall Resolved

Figure 3: Y+ and Velocity Contours for different approaches,Re=$2 * 10^6$

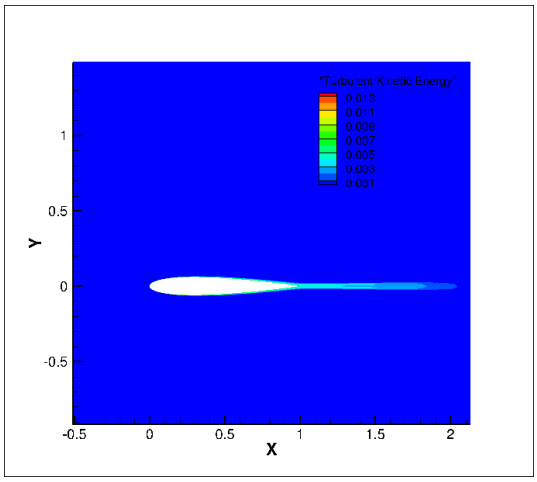

(a) Turbulent Kinetic Energy,Wall Function

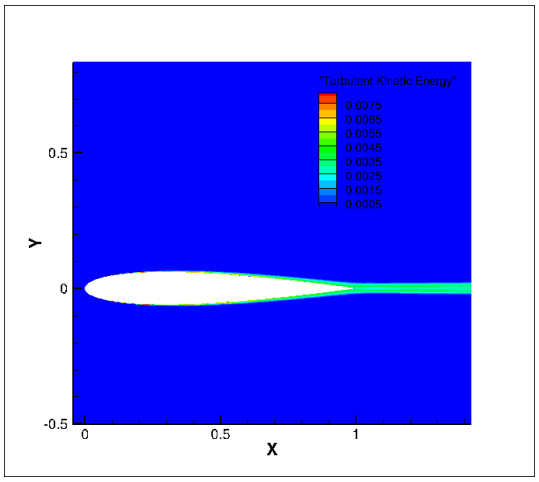

(b) Turbulent Kinetic Energy,Wall Resolved

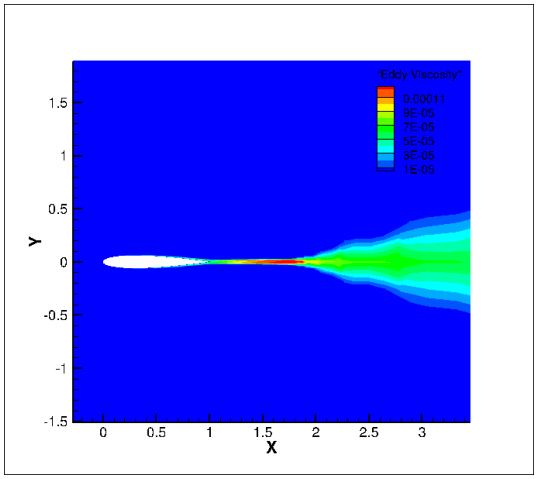

(c) Eddy Viscosity,Wall Function

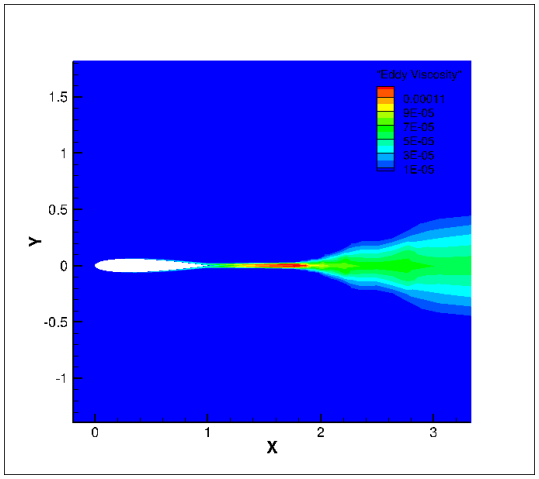

(d) Eddy Viscosity,Wall Resolved

Figure 4: Turbulent Kinetic Energy and Eddy Viscosity for different aprroaches,Re=$2 * 10^6$

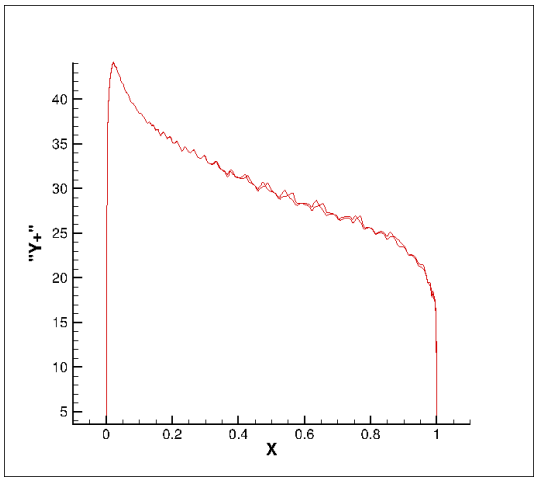

(a) Y+,Wall Function

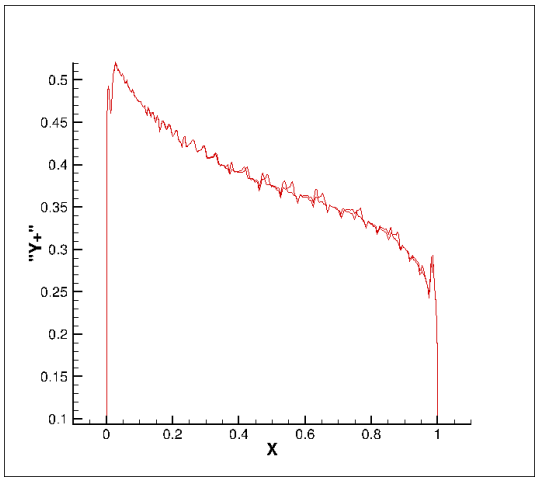

(b) Y+,Wall Resolved

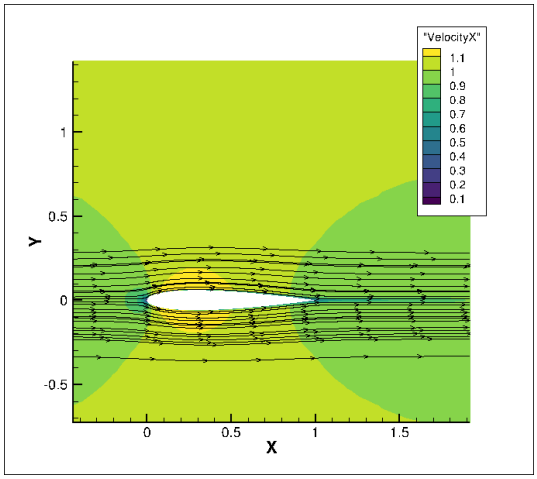

(c) Velocity,Wall Function

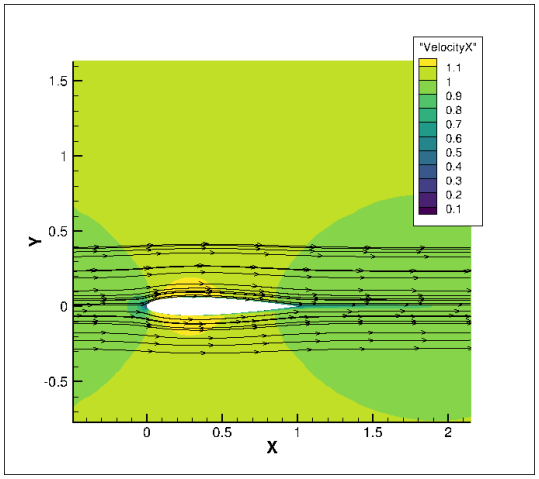

(d) Velocity,Wall Resolved

Figure 5: Y+ and Velocity Contours for different approaches,Re=$4 * 10^6$

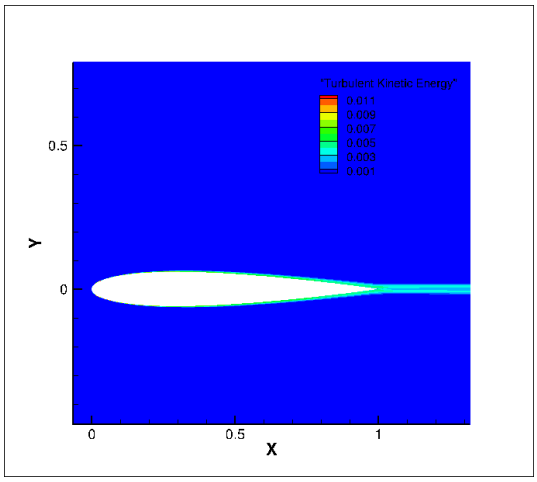

(a) Turbulent Kinetic Energy,Wall Function

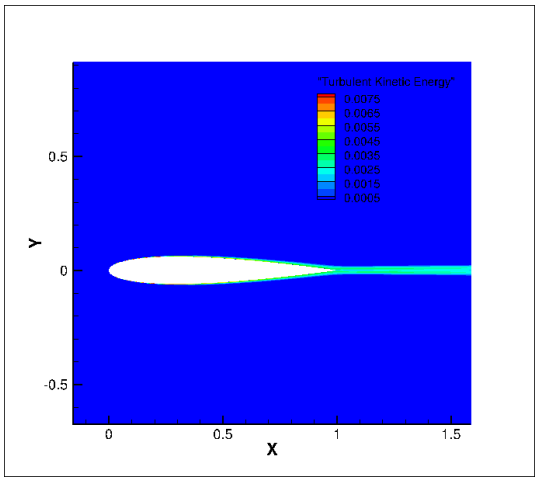

(b) Turbulent Kinetic Energy,Wall Resolved

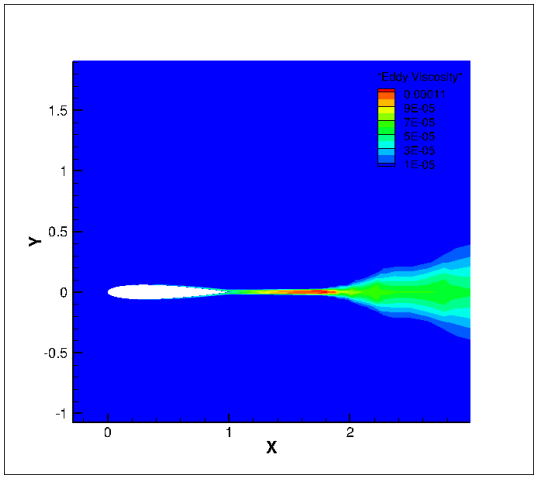

(c) Eddy Viscosity,Wall Function

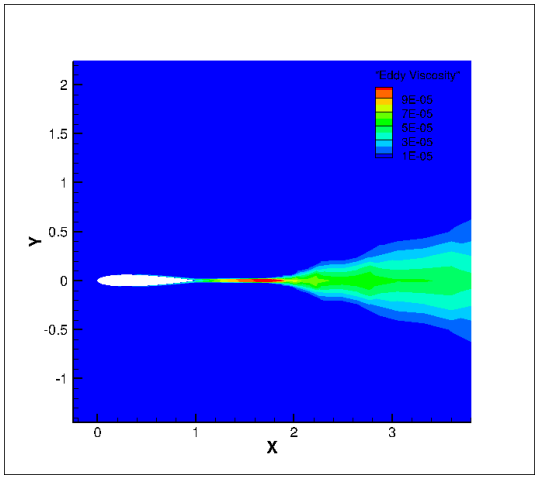

(d) Eddy Viscosity,Wall Resolved

Figure 6: Turbulent Kinetic Energy and Eddy Viscosity for different approaches,Re=$4 * 10^6$

2.3 Norm of the Velocity Vector

The below figures represents the velocity vector for the different approaches and the different Reynolds number.

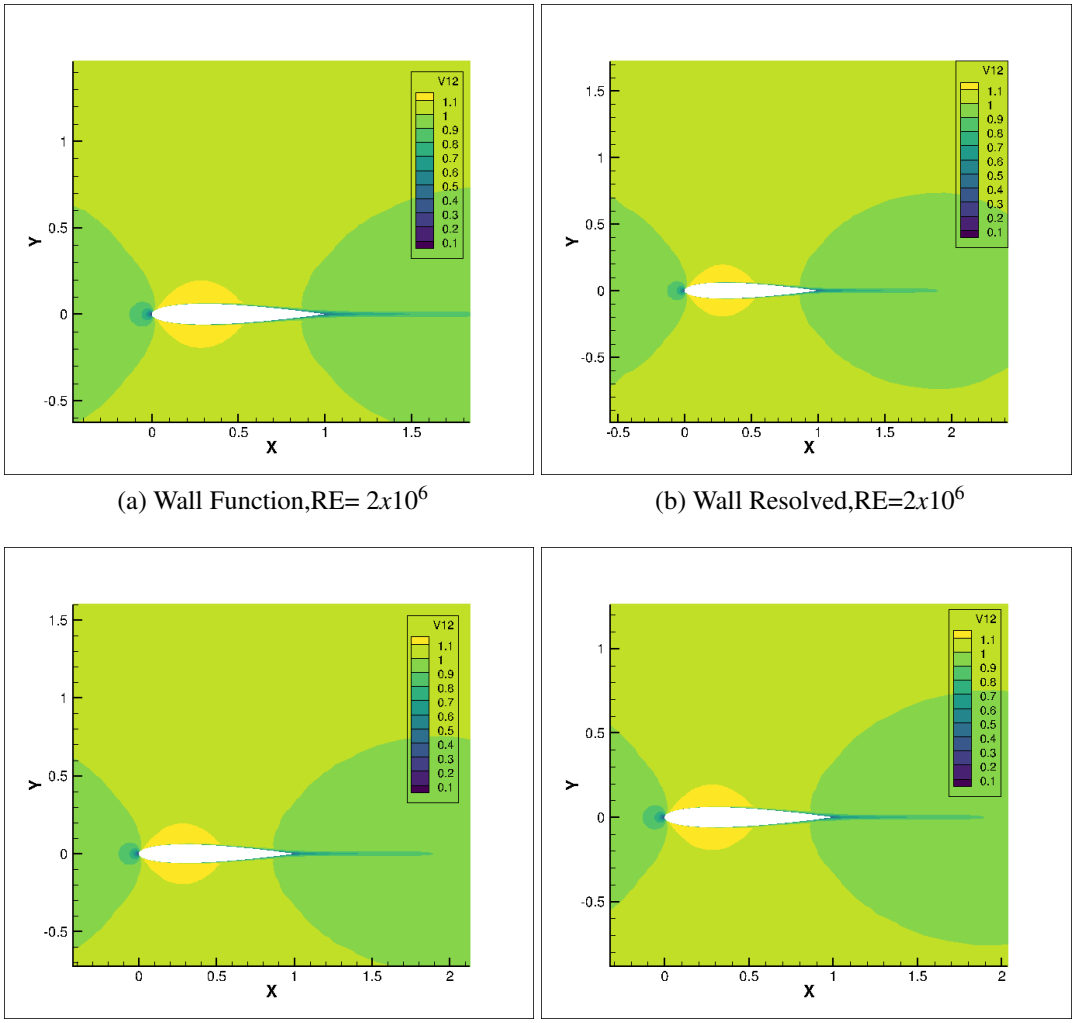

(a) Wall Function,RE= $2x10^6$

(b) Wall Resolved,RE=$2x10^6$

(c) Wall Function,RE= $4x10^6$

(d) [Wall Resolved,RE=$4x10^6$

Figure 7: Norm of the Velocity vector for different approaches and two Reynold's number

2.4 Drag Co-efficient (C_d) with Reynolds number

This subsection involves the study of the evolution of drag coefficient with increasing Reynolds number. The simulations are carried out at four increasing Re: $1x10^6, 2x10^6, 3x10^6 and 4x10^6$ .The computations are done on a medium grid adapted to both wall function and wall resolved approaches for the sake of comparison. These results are then validated with the experimental results from McCroskey, 1987.

The expression for drag force is,

$$F_x = \frac{1}{2} C_d \rho U^2 A$$

where,U is the stream velocity of the fluid,and the A is area of the body.By the assumptions and

the considerations made,the expressions becomes,

$$C_d = 2 * F_x$$

The below figure,shows the comparison of numerical and experimental results.forced. It can be observed that both wall function and wall resolved results matches with the experimental curve with trips as expected since it is the one for a turbulent flow and the numerical model used to solve assumes that the flow is fully turbulent throughout.

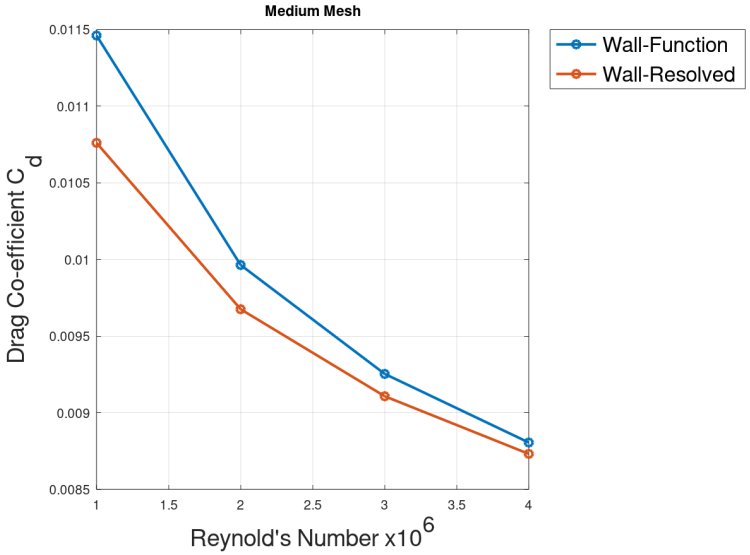

Figure 8: Evolution of Drag Coefficient

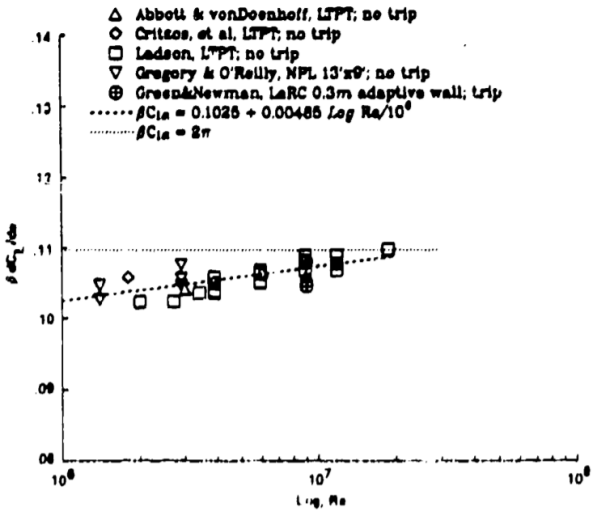

Figure 9: McCroskey 1987(C_p v/s Re)

2.5 Grid Convergence Study

In this section,we are going to study the convergence of the solution as the grid gets refined.The three meshes considered are coarse,medium and fine.The Reynolds number is at Re =$2x10^6$ using wall resolved approach.From the below figure,it can be ensured that Forces are converged and y+ values are around 0.5. To study the grid convergence,the Drag co-efficient was plotted

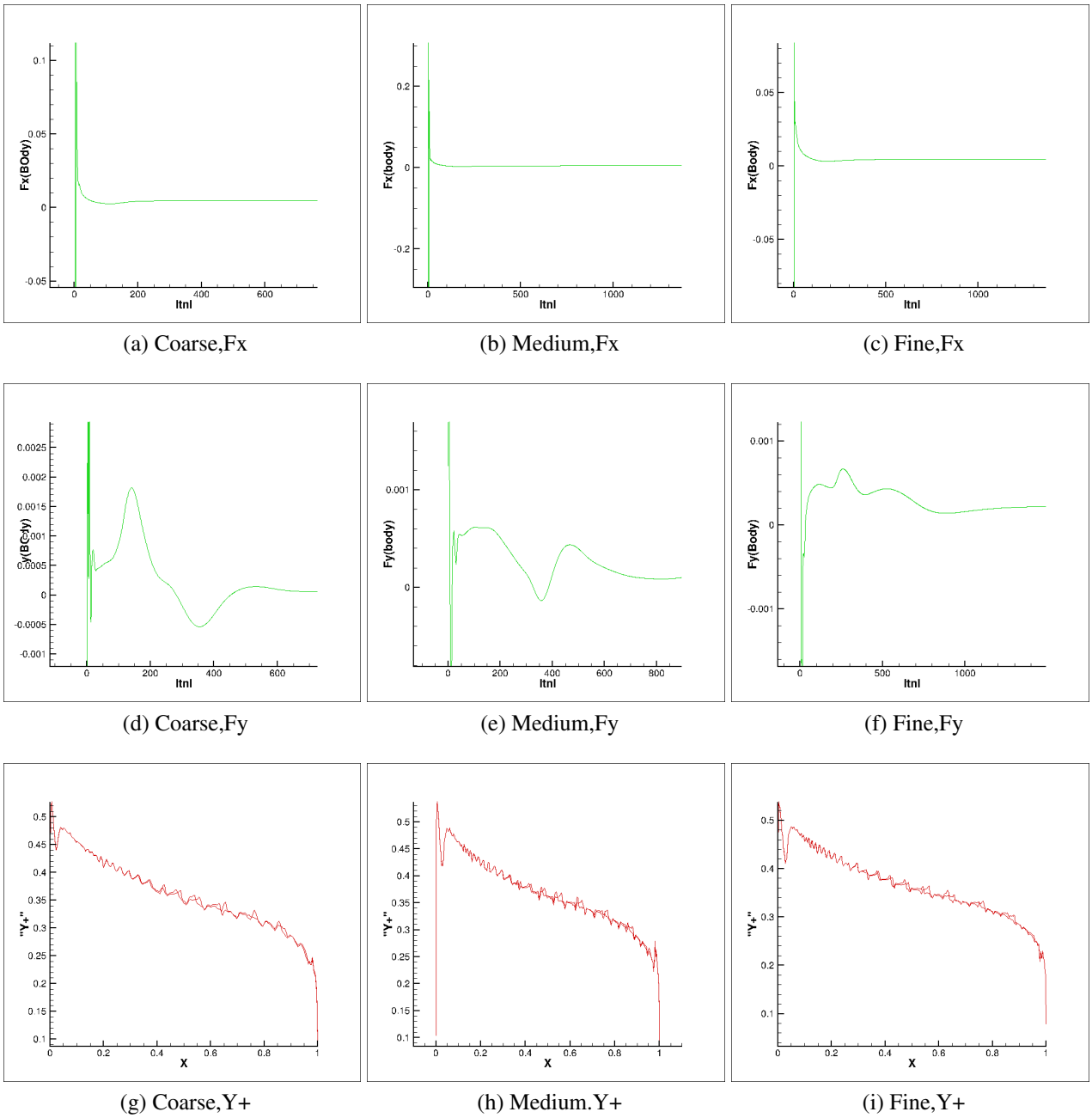

(a) Coarse,Fx (b) Medium,Fx (c) Fine,Fx

(d) Coarse,Fy (e) Medium,Fy (f) Fine,Fy

(g) Coarse,Y+ (h) Medium.Y+ (i) Fine,Y+

Figure 10: Check for Convergence for forces and checks for y+ for coarse,medium and Flap meshes,Re=$2 * 10^6$

against the number of cells in different order meshes.It can be seen clearly that the Drag co-efficient seems to converge as the mesh gets towards fine.The lift co-efficient is very low as the angle of attack is zero degrees.

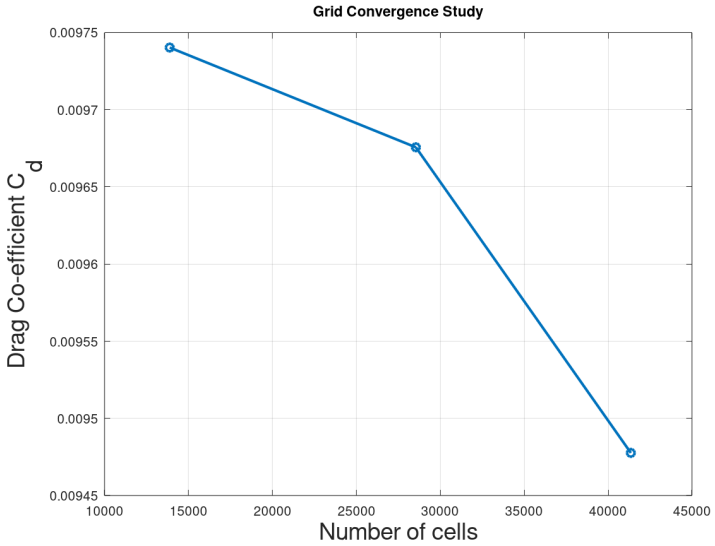

Figure 11: Evolution of Drag Coefficient with respect to number of cells

3 Part II :AGARD 303 test-case

In this section, the turbulent flow around a classical high-lift multiple-element airfoil in take-off configuration has been selected. The configuration is shown in the below figure. It consists of Slat, Main, and flap. The simulations are performed according to different flow conditions. The Reynolds number in all the cases is $3.52x10^6$. The angle of attack is 4.01 degrees. The turbulence approaches are Wall function and Wall resolved. The turbulence-free Euler approach is also used for comparison.

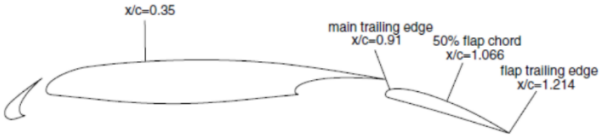

Figure 12: AGARD wing profile

3.1 Analysis with Wall function,Wall Resolved and Euler Approach

In this section, the simulations are performed with the three approaches on the medium grid. The flow fields are visualized and then compared with the experimental data. In the below figure, the medium meshes adapted to wall function, wall resolved and Euler approaches respectively that are used in the simulation. The Euler approach corresponds to a mesh without any viscous sub-layers, as there are no viscous effects to be taken care of close to the boundary due to zero viscosity. Slip boundary conditions are adopted for the Euler case.

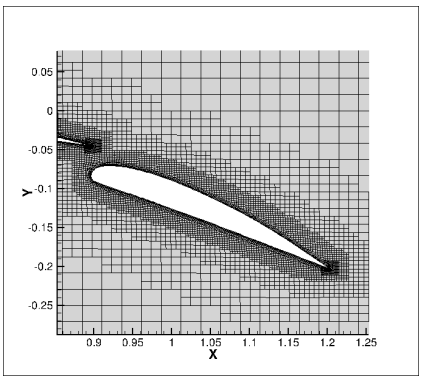

(a) Wall Function

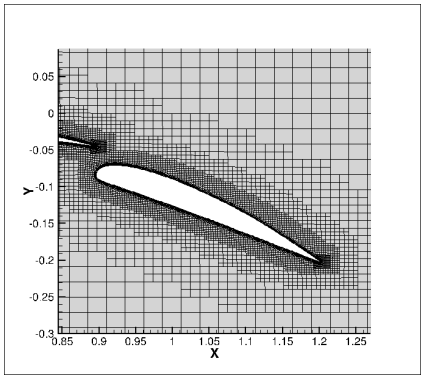

(b) Wall Resolved

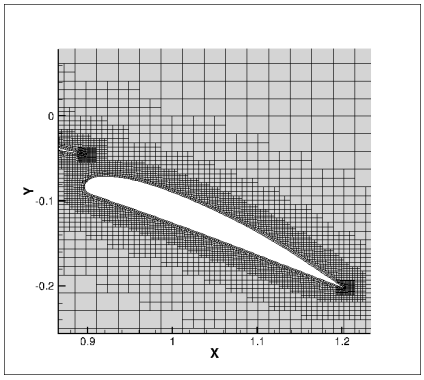

(c) Euler

Figure 13: Adapted Medium Meshes for different approaches

3.2 Y+ values,Convergence and the flow fields

It is checked to ensure that the forces and the residuals have converged well and also the y+ values are acceptable for the approach being used. The below figures illustrates the convergence of forces in each of the elements (Slat, Main, and Flap) for the different approaches considered. The below figures ensures that the y+ values are in the range for the approaches being used.

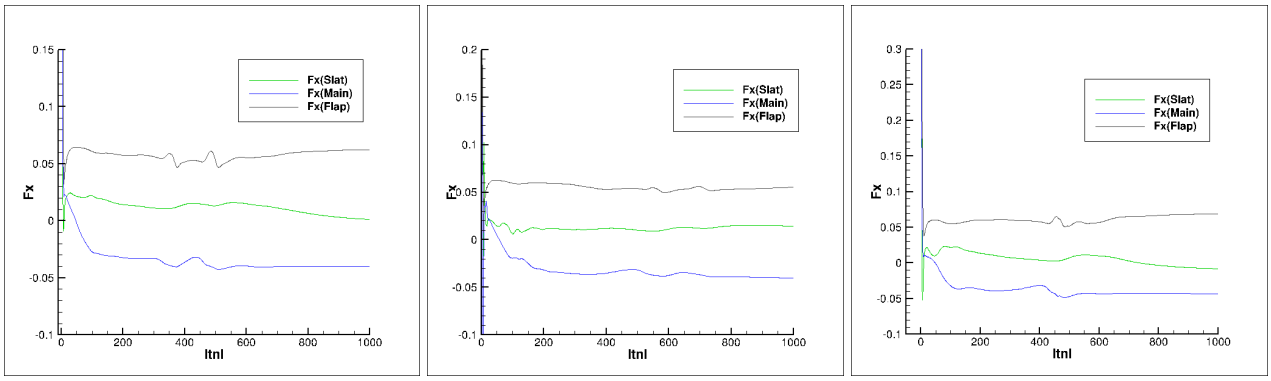

(a) Wall Function (b) Wall Resolved (c) Euler

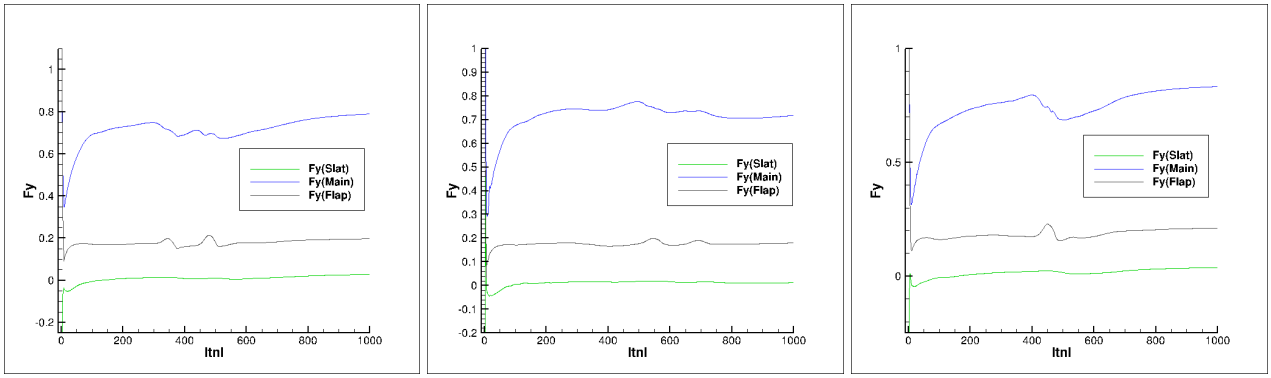

(d) Wall Function (e) Wall Resolved (f) Euler

Figure 14: Check for Convergence of forces

But, for the Euler approach, there is no y+, as no special wall treatment is adopted. So, only forces are ensured for this case. The y+ value for the wall resolved case close to the leading edge of the main element jumps past 1 due to the sudden suction or pressure drop on its upper surface which increases the velocity sharply. However, that should still be acceptable. Since 0.5 was used for this medium grid to adapt to wall resolved, using a much lower y+ value so that it remains < 1 for the maximum velocity experienced should avoid this issue. The below

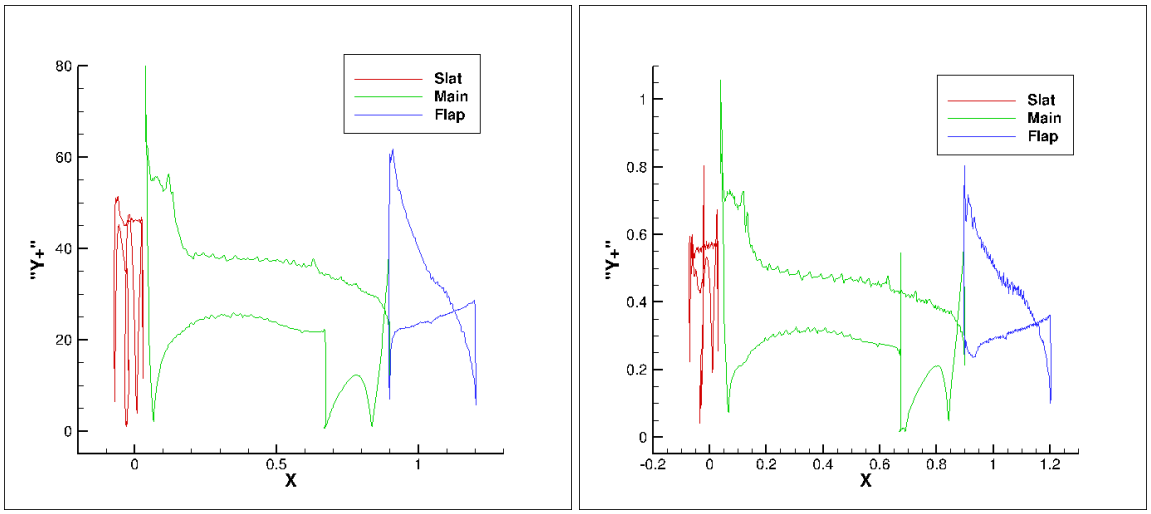

(a) Wall Function (b) Wall Resolved

Figure 15: Y+ values for different approaches for Medium mesh

figure illustrates the velocity field and Pressure from the wall function, wall resolved, and the Euler approach. respectively. Firstly, in all the figures, it is evident that the pressure drop close to the leading edge of the main element on the upper surface creates a suction that accelerates the fluid along the upper surface of the wing as observed in the figures. The pressure difference between the upper surface and the lower surface creates a lift force, and the major contribution comes from the main element close to its leading edge. This increased lift force is due to the increase in curvature of the airfoil provided by the adjustable slat at the front. Slats are hence used to generate extra lift force if needed especially during take-off.

The below figures, illustrate the turbulent viscosity from two approaches. Compared to the two approaches, the eddy viscosity field from the wall resolved one is slightly more intense, especially in the trailing edge of the main element and the one from the wall function approach seems to be diffusing a bit earlier close to the trailing edge of the flaps.

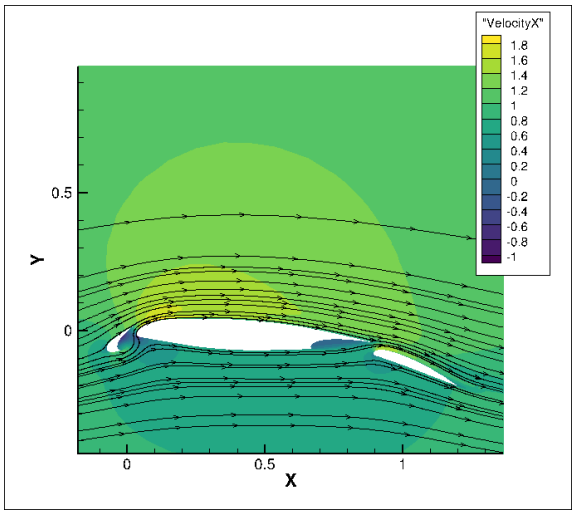

(a) Velocity,Wall Function

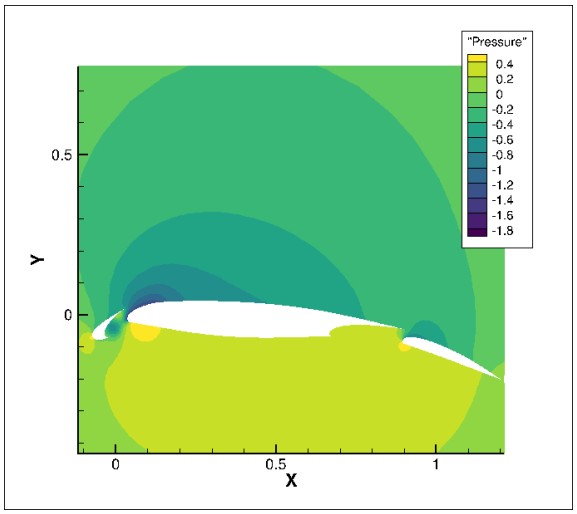

(b) Pressure,Wall Function

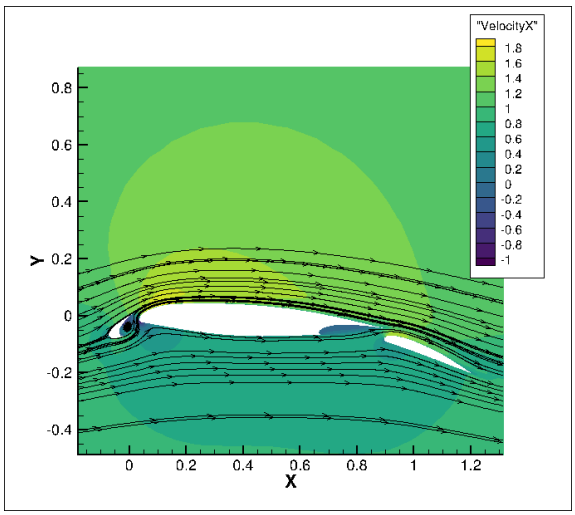

(c) Velocity,Wall Resolved

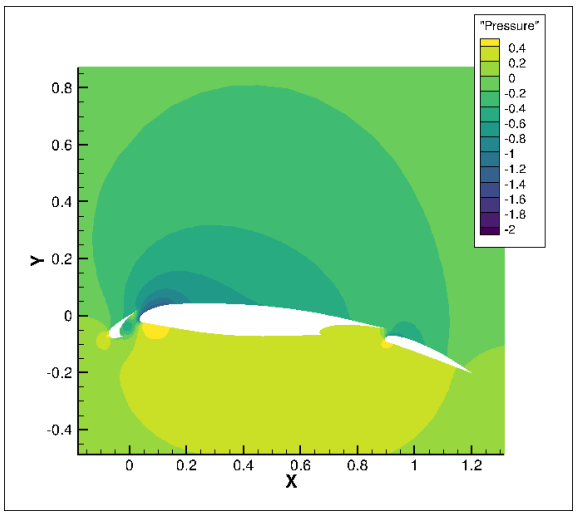

(d) Pressure,Wall Resolved

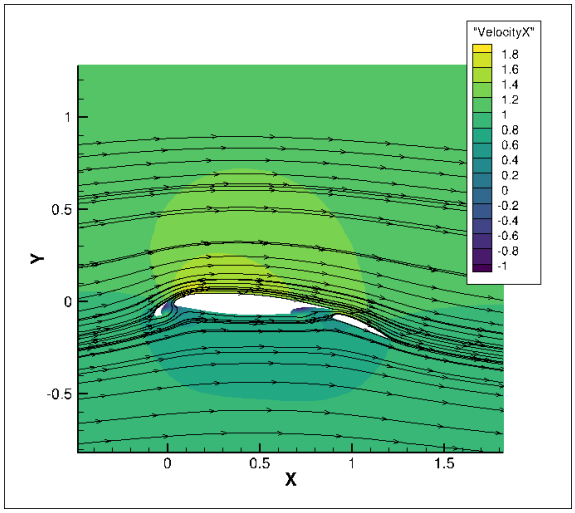

(e) Velocity,Euler

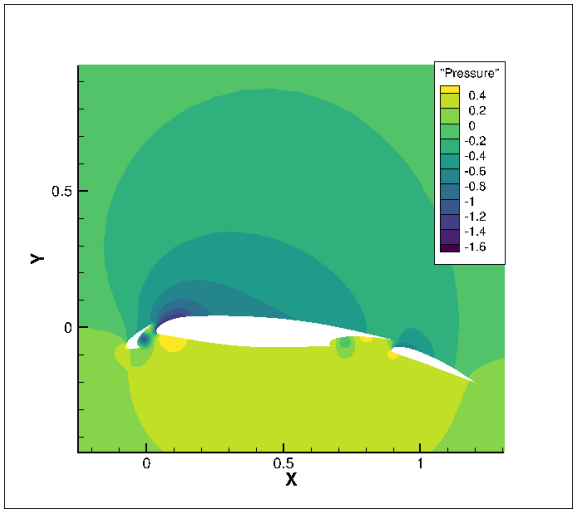

(f) Pressure,Euler

Figure 16: Velocity and Pressure Contours for different approaches

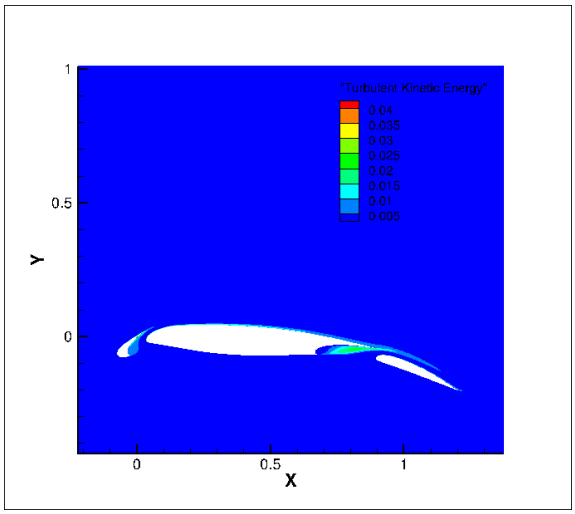

(a) Turbulent Kinetic Energy,Wall Function

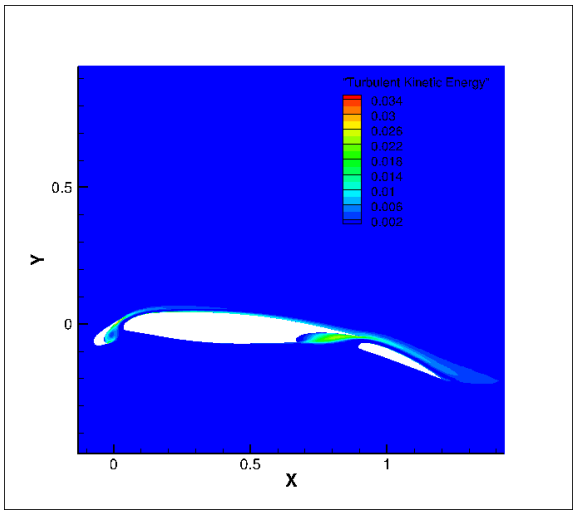

(b) Turbulent Kinetic Energy,Wall Resolved

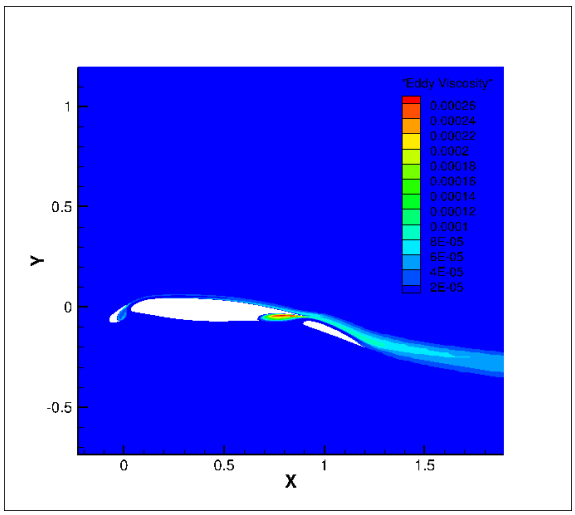

(c) Eddy Viscosity,Wall Function

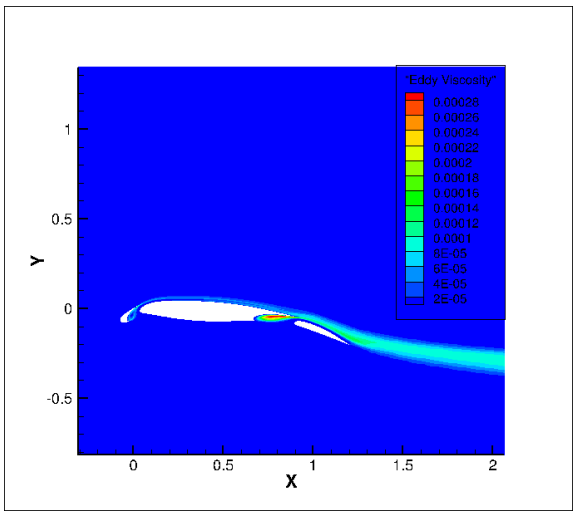

(d) Eddy Viscosity,Wall Resolved

Figure 17: Eddy Viscosity and Turbulent Kinetic Energy for two turbulent approach

3.3 Comparison with Experimental Results

In this section,We are going to compare the pressure coefficient (C_p) along the body,computed for the three approaches with the experimental results.The total pressure profile is compared at 4 different locations as shown in the below figures. It can be observed from the above

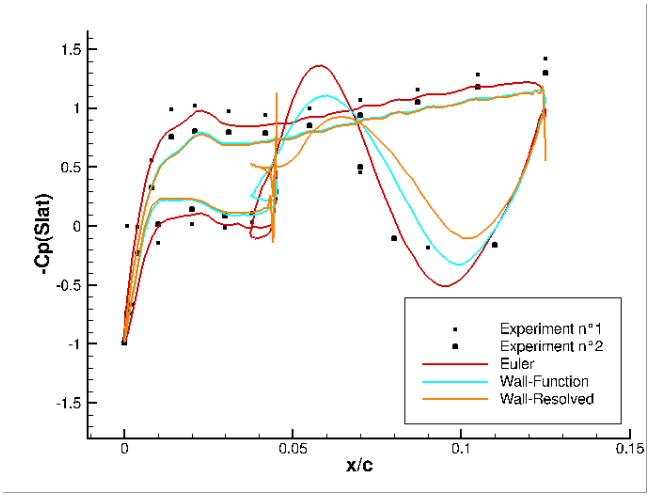

Figure 18: Comparison of Cp-Slat with Experimental values

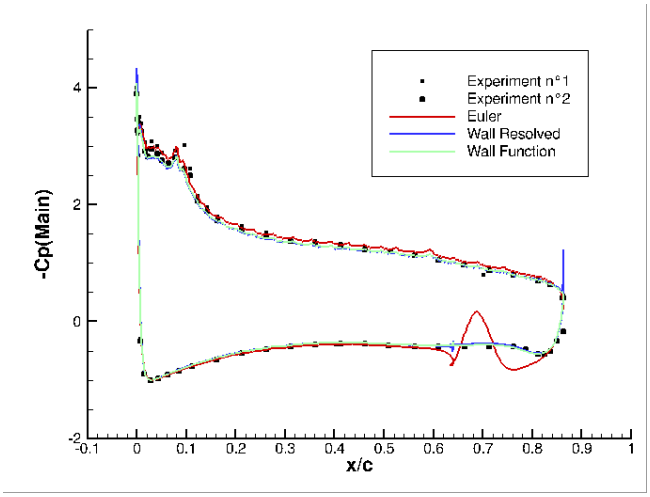

Figure 19: Comparison of Cp-Main with Experimental values

approaches, the obtained results seem to match well with the experimental values. But there is some discrepancy in the Slat comparison. but, they agree mostly. Among the three approaches, the wall resolved approach seems to give the least discrepancy, followed by the wall function and then the non-turbulent Euler approach as expected since the experimental results are for a turbulent flow.

The above figure indicates the comparison with the experimental results of the pressure profiles extracted at four different locations along the body.

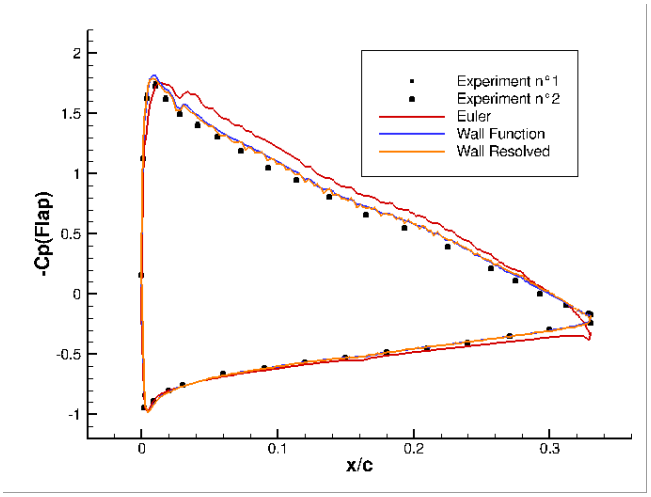

Figure 20: Comparison of Cp-Flap with Experimental values

3.4 Comparison of Drag and Lift coefficients

The Drag and Lift coefficients are expressed as,

$$C_d = \frac{F_x^{Slat} + F_x^{Main} + F_x^{Flap}}{0.5\rho U^2 A}$$

$$C_L = \frac{F_y^{Slat} + F_y^{Main} + F_y^{Flap}}{0.5\rho U^2 A}$$

Where,ρ is the density of the fluid ,which is set to 1.Area is set to 1 and the U is the free stream velocity is set to 1.

The below table represents the drag and lift co-efficient for different approaches.

Approach	**Drag**(C_d)	**Lift**(C_L)
Wall function	0.21241	2.075611
Wall resolved	0.212268	2.086285
Euler	0.251522	2.223532

Table 1: Comparison of Drag and Lift Coefficients for medium grid mesh

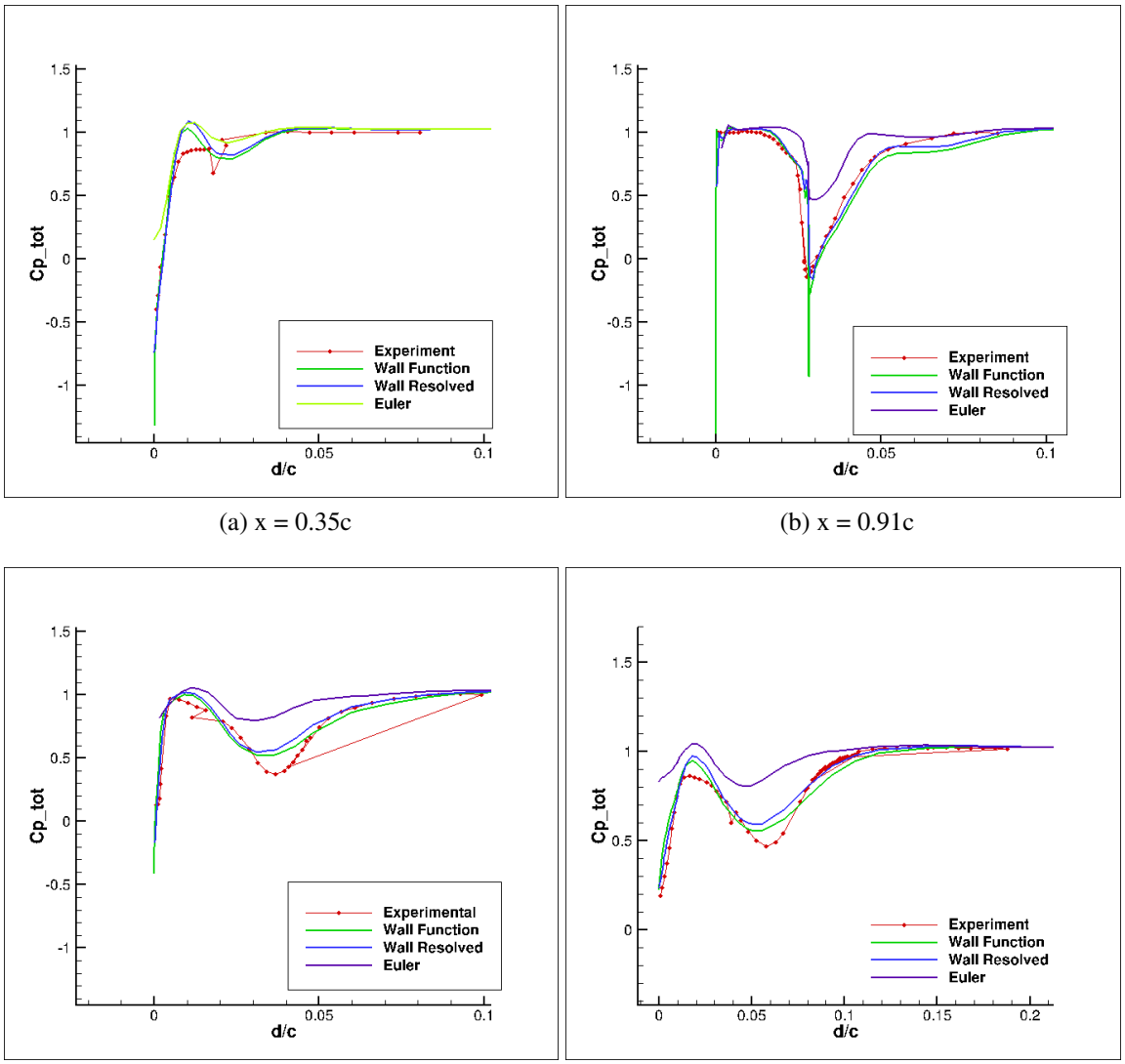

(a) x = 0.35c

(b) x = 0.91c

(c) x = 1.066c

(d) x = 1.214c

Figure 21: Comparison of total pressure profiles at different locations

3.5 Grid Convergence Study

In this section,we are going to study,the wall resolved approach by checking the convergence of the drag and lift coefficients for Coarse,Medium and Fine mesh.From the below figures,it can be ensured that the forces have converged and the y+ values are in acceptable range. The below figure,shows the grid convergence for different number of mesh cells for both Drag and Lift Co-efficient.

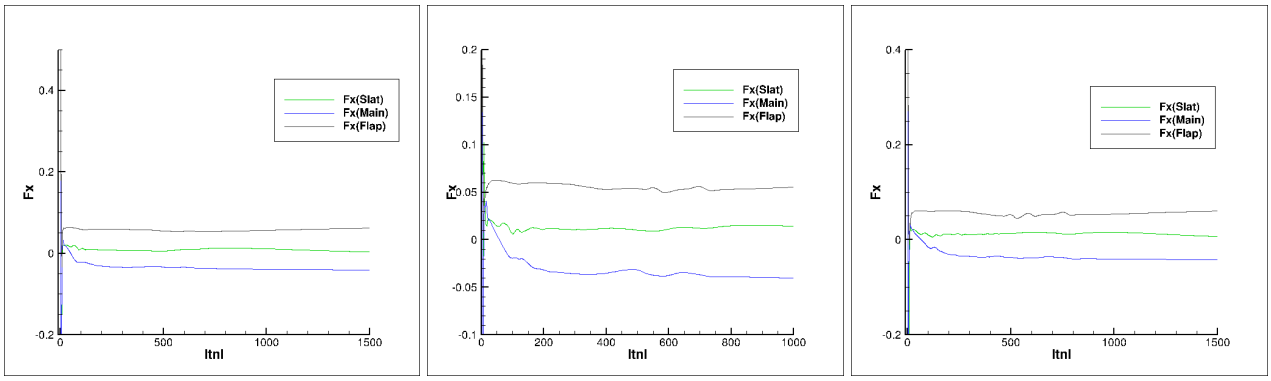

(a) Fx,Coarse (b) Fx,Medium (c) Fx,Fine

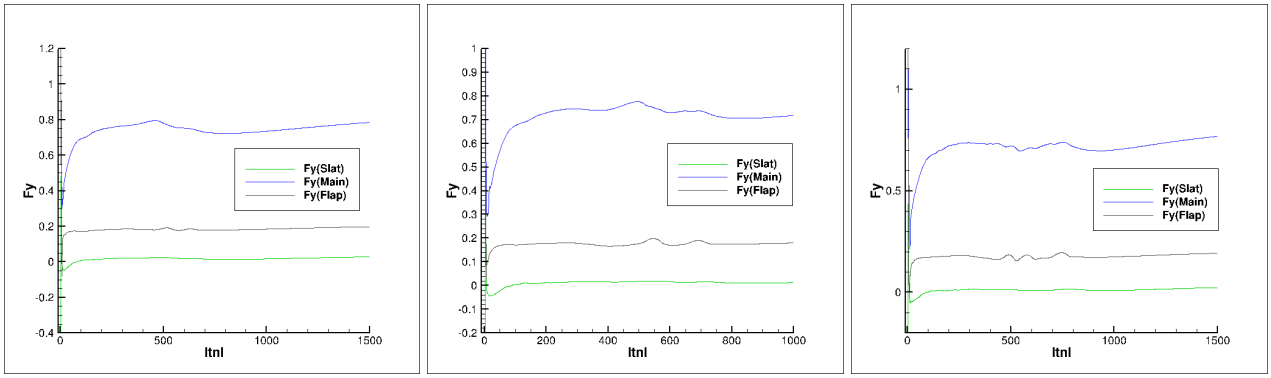

(d) Fy,Coarse (e) Fy,Medium (f) Fy,Fine

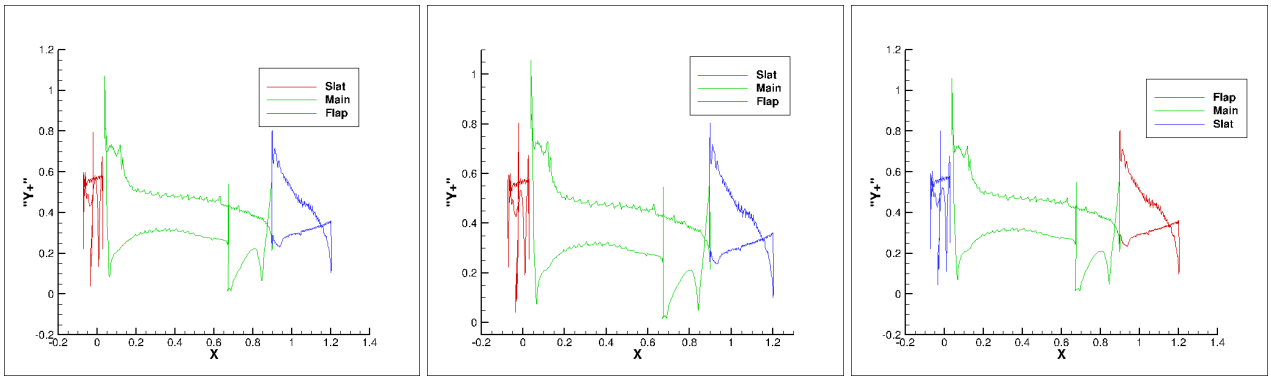

(g) Y+,Coarse (h) Y+,Medium (i) Y+.Fine

Figure 22: Checks for convergence of forces and residuals,and y+ for all the meshes adapted to wall resolved

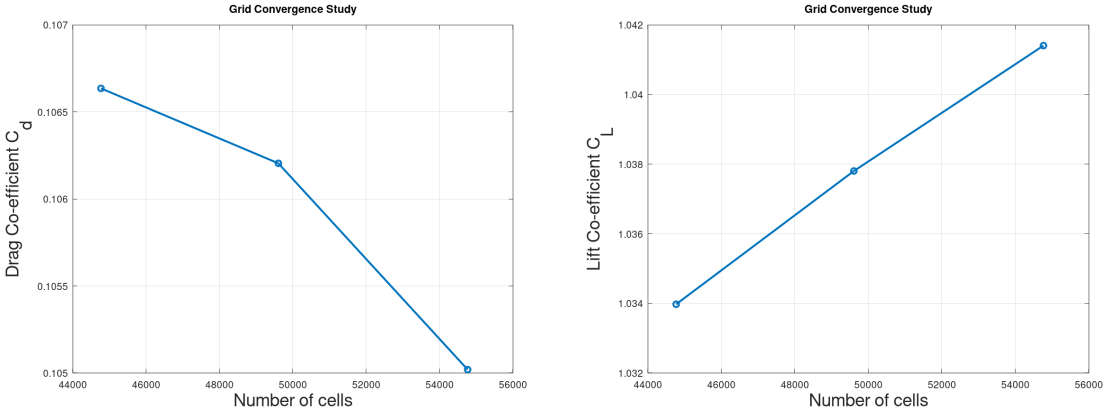

(a) x = 0.35c (b) x = 0.91c

Figure 23: Convergence of Drag and Lift Co-efficients

3.6 Influece of Numerical Parameter

3.6.1 Effect of the Upwind Scheme

The default scheme used in Fine/Marine is AVLSMART.AVLSMART. In this study, we use a first-order upwind differencing scheme (UDS) instead and compare it with the default case to analyze their effects on the prediction of turbulent quantities such as the eddy viscosity and the turbulent kinetic energy. The below figures illustrates the Turbulent kinetic energies and Eddy viscosity for AVLSMART and upwind scheme respectively. It is evident near the main trailing edge and in the wake of the wing that the eddy viscosity and the turbulent kinetic energy predicted using the AVLSMART scheme are more intense compared to the one predicted by the Upwind scheme. The upwind scheme seems to underestimate or diffuse the turbulent quantity. Smearing of the quantities is observed.

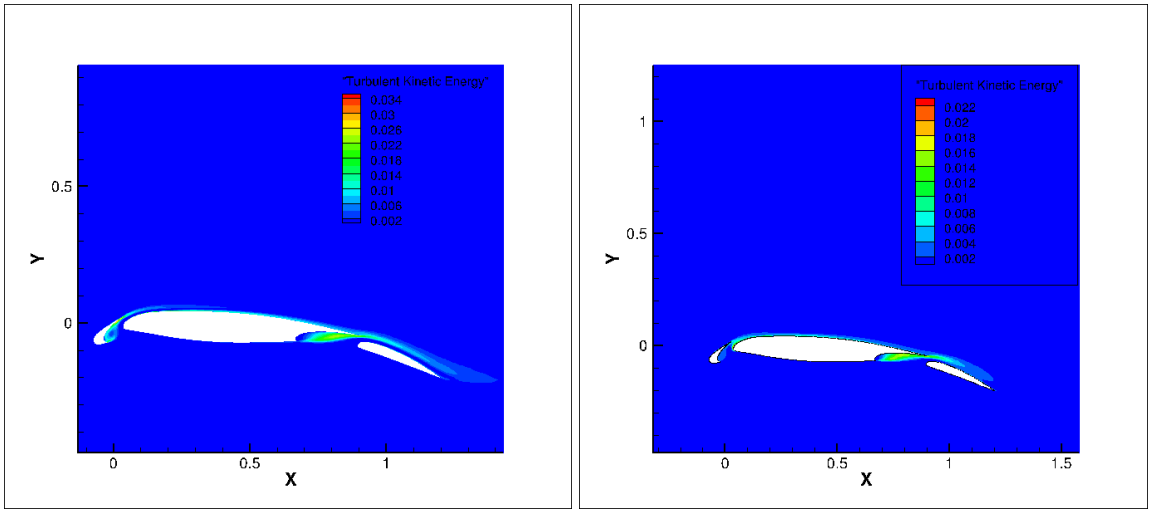

(a) Turbulent Kinetic Energy,AVLSMART

(b) Turbulent Kinetic Energy,Upwind

(c) Eddy Viscosity,AVLSMART

(d) Eddy Viscosity,Upwind

Figure 24: Comparison of the turbulent Kinetic energy and Eddy Viscosity for two discretisation schemes

3.7 Effect of Under Relaxation

Under relaxation is used to slow down steep changes in the solution between the iterations and thus preserving the stability and ensuring the convergence. But it takes more iterations and time to converge. If the Relaxation parameter is higher, the speed of the convergence is faster. However, there could be stability issues and chances of divergence of the solution. To study the effect of the under relaxation parameter, the Velocity component V_x and V_y are changed to 0.3 and the pressure to 0.2

The below figure shows the residual vs Non-linear iteration for different Under-relax Parameters. It can be shown that the converged solution is independent of the relaxation parameter chosen.

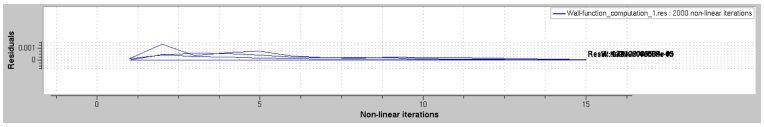

Figure 25: Residual vs Non-Linear Iterations for default parameters

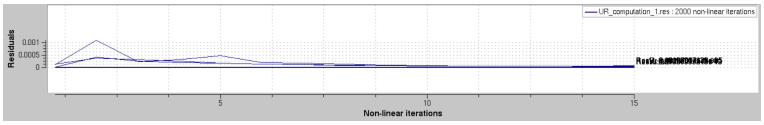

Figure 26: Residual vs Non-Linear Iterations for V_x and V_y are changed to 0.3 and the pressure to 0.2